Magnetic Field – Assisted Laser Ablation of Titanium Dioxide Nanoparticles in Water for Anti-Bacterial Applications

Hasan H. Bahjat
University of Technology
R.A. Ismail (raidismail@yahoo.com)
University of Technology, Iraq https://orcid.org/0000-0002-6629-3630
Ghassan M. Sulaiman
University of Technology
Majid S. Jabir
University of Technology

Original Research Full Papers

Keywords: TiO2 nanoparticles, Laser ablation, Water, Magnetic field, Antibacterial

Posted Date: February 10th, 2021

DOI: https://doi.org/10.21203/rs.3.rs-176836/v1

Version of Record: A version of this preprint was published at Journal of Inorganic and Organometallic Polymers and Materials on March 27th, 2021. See the published version at https://doi.org/10.1007/s10904-021-01973-8.

Abstract

Titanium oxide nanoparticles (TiO_2) were produced by pulsed Nd:YAG laser ablation in water under the effect of an external magnetic field. Various techniques such as X-ray diffraction (XRD), field emission scanning electron microscopy (FESEM), energy Dispersive x-ray (EDX), transmission electron microscopy (TEM), UV-Vis spectroscopy, and Raman spectroscopy were used to characterize the TiO_2 nanoparticles. The XRD analysis of titanium oxide nanoparticles revealed that the synthesized nanoparticles were polycrystalline with mixed of tetragonal anatase and rutile TiO_2. Scanning electron microscope shows the formation of spherical nanoparticles and the particles agglomeration decreases and the particle size from increases from 25nm to 35nm when the magnetic field applied. The optical energy gap of TiO_2 nanoparticles decreased from 4.6eV to 3.4eV after using the magnetic field during the ablation. Raman studies show the existence of five vibration modes belong to TiO_2. The antibacterial effect assay revealed a largest inhibition zone in *S. aureus* and *E. coli*, with a more potent effect for TiO_2 NPs prepared by magnetic field when compared with that prepared without presence of magnetic field.

1. Introduction

Nanomaterials have been drawn attention due to their unique optical and electronic properties as compared to those for bulk state [1]. These novel properties of this class of materials make those really promising for many of industrial, technological, and biomedical uses [2, 3, 4].

The demand for materials with antibacterial properties have been growing annually in different sectors such as textiles, food, water disinfection, medicine, and food packaging [5, 6, 7]. The increased resistance of some bacteria to some antibiotics and the toxicity to the human body of some organic antimicrobial substances has increased the interest in the development of inorganic antimicrobial substances. Among these compounds, metal and metal oxide compounds have attracted significant attention due to their broad-spectrum antibacterial activities. During last years, metal oxide nanoparticles, such as nickle oxide (NiO), zinc oxide (ZnO), copper oxide (CuO), and iron oxide (Fe_2O_3), have been extensively in biological applications due to their unique physiochemical properties [8, 9, 10]. Among metal oxide antimicrobial agents, TiO2 is a valuable semiconducting transition metal oxide material and shows special features, such as easy control, reduced cost, non-toxicity, and good resistance to chemical erosion, that allow its application in optics, solar cells, chemical sensors, electronics, antibacterial agents. In general, TiO_2 has three important phases anatase (tetragonal), rutile (tetragonal) and brookite {orthorhombic) [11].

Several methods have been used to synthesis TiO_2 nanoparticles such as wet-chemical synthesis, reverse micelles, metal organic chemical vapor deposition, sol–gel, solvothermal, microemulsion, electrochemical, and laser ablation in liquid [12–13]. Pulsed-laser ablation method in liquid (PLAL) is considering one of the promising techniques for production of highly colloidal monodispersed nanoparticles.

PLAL is a technique at which the high intensity laser irradiates metal ormetal oxide target immersed in liquid. PLAL exhibits many features such as stability of the product, low cost, high purity, simplicity, no vacuum needed, good control on the size and morphology of the product. InPLAL technique,the control on properties of the synthesized particles can be achieved by variation the laser parameters such as laser wavelength, laser energy density, pulses repetition rate, pulse duration [14].The solution type is also affecting the concentration, morphology and size of the nanoparticles.Nath et al. prepared TiO2 nanoparticles by laser ablation in water and the synthesized nanoparticles with size ranged from 2 to 45nm with energy gap of 3eV [15]. Singh et al. studied the properties of TiO2 nanoparticles synthesized by nanoseconds of 8W fiber laser ablation of Ti target in deionized water [14 – 11]. The effect of liquid ablation type namely, water, acetone and CTAB on the characteristics of TiO_2 nanoparticles prepared by laser ablation was studied by Solati et al. [16].

Applying the magnetic field during the preparation of the nanoparticles has drawn attention due to the control on the morphology, size and crystallinity of the nanoparticles. Attan et al. prepared well-aligned TiO_2 nanowires by sol-gel method under effect of magnetic field of 9.4T [17]. Until now, only limited information is available on the potential toxicity of TiO_2 prepared by magnetic field to bacterial growth. Thus, the present study was designed for preparation of TiO_2 nanoparticles by magnetic field –assisted laser ablation in liquid MFALAL technique and evaluate its antibacterial performance on both Gram-positive and Gram- negative bacterial organisms [18].

2. Materials And Methods

2.1. Materials

Titanium oxide powder (TiO_2) with 99.9% purity (Merk, India) were used at analytical grade. Water was double distilled with Millipore water purification system.

2.2. Preparation of TiO_2 nanoparticles

Titanium oxide nanoparticles were produced by laser ablation of titanium oxide pellet in deionized water. The pellet was made by pressing the TiO_2 powder with purity of 99.9% supplied from using hydraulic compressor. The pellet immersed in glass vessel contained deionized water and the height of the water above the target is adjusted to be around 3mm.Laser ablation process was carried out using Nd- YAG operating at wavelength of 1064 nm and the laser fluence used for the ablation was6J/cm^2 at 1Hz repetition frequency. The laser beam was focused on the TiO_2 pellet by using positive lens with a focal length of 8cm and the spot size on the pellet was 0.3mm. To carry out the laser ablation under effect of magnetic field, two rectangular magnets with 1.2T was applied parallel to the laser as shown in Fig. 1.

2.3. Characterization of TiO_2 nanoparticles

The field emission scan electron microscopy (FE-SEM) was conducted using JSM-IT800 (origin) equipped with energy dispersive x-ray EDX to examine the morphology and the chemical composition of prepared nanoparticles was used. Transmission electron microscope (TEM; Tecnai G2 20 S-TWIN, China) was used to study the morphology and the size of TiO_2nanoparticles. The optical absorption of the colloidal nanoparticles was measured by double-beam UV-VIS spectrophotometer model (Metertech, SP8001 spectrophotometer, Japan) and the structure of the nanoparticles was studied by x-ray diffraction (Philips PW, Japan).Raman spectroscopy (BrukerSenterra Raman microscope)was employed to examine the vibration modes of TiO_2 nanoparticles.

2.5. Anti-bacterial activity assay of TiO_2 nanoparticles

Anti-bacterial activity of TiO2 NPs was examined against two clinical isolates like *Escherichia coli* (gram-negative) and *Staphylococcus aureus* (gram-positive). The stock cultures for these two bacterial isolates was transferred into Mueller Hinton agar medium, incubated over night at 37° C, and stored in refrigerator at 4° C until used. The antibacterial activity of TiO_2 NPs was inspected by utilizing well dissemination procedure [19]. Wells with diameters of about 6mm were made at the surface of agar media by tips of micropipette, then NPs suspensions with different concentrations were added into the wells. These plates were kept at the incubator for 24 hours. The antibacterial effectiveness of TiO_2 NPs was recorded by measuring inhibition zone diameters from different directions using a ruler more than once. All tests were performed in duplicates and refined water was utilized as a negative control treatment.

3. Results And Discussion

Fig.2 shows the XRD pattern of TiO_2 nanoparticles prepared without and with the presence of the magnetic field. Fourteen XRD peaks located at 2Θ = 25.7° , 27.4°, 29.3°, 32.9°,36.1°, 37.7°, 41.2°, 44.1°, 45.5°, 50.2°, 54.4°, 56.6°, 61.2° and 72.3° corresponding to (220), (110), (131), (230), (011), (232), (111), (120), (242), (250), (211), (220), (022) and (131) plane, respectively, were observed for TiO_2 prepared without magnetic field. These peaks are indexed to crystalline rutile (R), anatase (A) and panguite (P) TiO_2. After applying an external magnetic field, it observed that some difference in the shape of the XRD peaks and appearance of new XRD peaks at 22.2°, 23.8°, 31.5° and 37° corresponded to (021), (211), (222) and (011) plane which related to rutile and panguite TiO_2. This could be due to the improvement in the crystallinity of the nanoparticles since the nanoparticles have been highly oriented along (110) plane after applying the magnetic field during the preparation of the nanoparticles. The magnetic field plays an important role in the enhancement of alignment and orientations of the molecules and domains. The crystal structure of TiO_2 NPs prepared with and without magnetic field are shown in Fig.3 which are agree with reported results of rutile TiO_2 [20-22].

The FESEM images of TiO_2 nanoparticles prepared with and without magnetic field are shown in Fig.4.The sample prepared without magnetic field exhibits spherical nanoparticles with average particle size of 29 nm and some agglomerated nanoparticles have been observed. The reason of the

agglomeration could be ascribed to the high surface energy of the nanoparticles [16]. After applying of the magnetic field, the FESEM image revealed that the morphology of the nanoparticles was changed from nanoparticles to platelets-like morphology and the magnified SEM image showed some of spherical nanoparticles and nanowires were attached to the nanoplates. The change in the morphology may due to the increasing of the plasma confinement when applying the magnetic field during the laser ablation [23].

The particle size (d) of the TiO_2 was determined from optical properties using the following Brus equation

$$E_g^* = E_g^{Bulk} + \frac{\hbar^2\pi^2}{2d^2}\left(\frac{1}{m_e^*} + \frac{1}{m_h^*}\right) \quad (1)$$

Where E_g* is the energy gap of TiO_2 nanoparticles, E_g Bulk is the energy gap of bulk TiO_2 which is taken 3.2eV, m_{*e} is the effective mass of electron of TiO_2 and it is taken $0.09m_o$, m^*_h is the effective mass of hole of TiO_2 and it is taken $0.56m_o$ [24]. After substituting all the values in Eq.1, the particle size was calculated and found to be 4nm for TiO_2 prepared at B = 0 and 22nm for TiO_2 nanoparticles synthesized at B = 1.2T. These values are smaller than of those determined from SEM investigation. Fig.5 shows the EDX spectra of TiO_2 nanoparticles. We have observed the presence of peaks related to oxygen and titanium elements and the peaks of other elements are belonged to the substrate.

Fig.6 shows the TEM images of TiO_2 NPs synthesized with and without magnetic field. It is obvious that the nanoparticles prepared without magnetic field have spherical shape with average size of 25nm and transformed to high concentration of nanowires when a magnetic field applied during laser ablation. We think that formation of nanowires can be ascribed to that the magnetized nanoparticles are attracting each other and resulted in the formation linear chains along the magnetic lines.

The optical absorption of TiO_2 nanoparticle is shown in Fig.7-a. As shown, applying of the magnetic field during the ablation process has increased the optical absorption due to the formation of platelets and nanowires morphologies as well as to the increasing the concentration of TiO_2. Due to the enhancement in the plasma confinement, the plasma temperature increased when the magnetic field applied which resulted in the formation of high concentration of TiO_2 nanowires. A small peak was observed at 270nm which can be attributed to the quantum size effect [24, 25].

The optical energy gap of TiO_2 nanoparticles was determined by plottingof $(\alpha h\nu)^2$ versus photon energy for direct transition as shown in Fig.7-b and the extrapolation of the linear partto the$(\alpha h\nu)^2$ =0 point gives the direct optical energy gap [26,27]. Fig.6-b reveals the energy gap of TiO_2 nanoparticles prepared with and without magnetic field were 3.4 and 4.6 eV, respectively. The TiO_2 sample prepared without magnetic field has energy gap larger than that of TiO_2 sample prepared with magnetic field. This could be ascribed to the effect of the particle size of TiO_2 which in good agreement with results of FE-SEM and TEM. The energy gap obtained values is relatively is larger than those of TiO_2 nanoparticles prepared by other techniques due to the selecting of optimum laser fluence [28].

Raman spectra of titanium oxide nanoparticles produced without and with magnetic field are shown in Fig.8. We have detected five vibration modes for sample prepared with magnetic field located at148cm^{-1} is indexed to B_{1g}, the peak found at 197cm^{-1} is belonged to E_g. The peak at 244cm^{-1} is related to the second order effect and the peak located at 477 cm^{-1} is belonged to E_g. We have also found Raman peak 555cm^{-1} which is can be indexed to B_{1g}. Strong Raman peak was found at 603cm^{-1} is related to A_{1g} mode. Finally, Raman peak was noticed at 802cm^{-1} which related to B_{2g}. These results are consistent with those reported in literatures [30, 31]. Applying the magnetic field leads to increasing the intensity of Raman peaks and no shift in Raman peaks was noticed for TiO_2 nanoparticles prepared under magnetic field.

Antibacterial effect Table 1 and Figure 9 appear the antibacterial impact of the fabricated TiO_2 NPs. The impact of TiO_2 NPs was more self-evident on the growth of *S. aureus* and *E. coli* for samples prepared with the effect of external magnetic field with inhibition zone reach to 34.8 mm and 33.6 mm, respectively. A moderately lower antibacterial impact was watched for TiO_2 NPs prepared without the effect of external magnetic field on the growth of *S. aureus* and *E. coli*, with the zone of hindrance that come to 26.8 mm and 29.2 mm, respectively. There was no significant effect between the bacterial species, but the significant appeared between the material prepared with the presence of a magnetic field and the absence of the field wandering during the preparation. The same picture was drowning in TiO_2 NPs synthesized without magnetic field. NPs have a specific property for antibacterial effectiveness against both Gram positive and Gram negative bacteria, as in the effectiveness of TiO_2 NPs in preventing the growth of *S. aureus* [32]. The mechanisms of the activity of the nanoparticle might occur in two successive stages; firstly, by causing damages in the outer membrane of the bacterial cell wall through electrostatic or direct interaction between the cell wall the NP. Secondly, by producing an active oxygen environment known as oxidative stress, e.g. during production of H_2O_2, because of the presence of metal oxides [33]. Other explanation for antibacterial activity may be was due to their effects on cell viability which are associated with damages to the mitochondrial enzymes and proteins of cell cycle. This higher effectiveness can be also explained by the ability of NPs to generate ROS even in the absence of light that can cause changes in macromolecules such as proteins, nuclei acids, and lipids by effects of oxidative stress. These oxygen species produce free radicals that are short lived and unstable, which influences nuclear viability and healthiness and finally leads to cell death. ROS can cause oxidation of proteins and peroxidation of lipids that leads to damaging the hardness of the cell membrane, changing permeability of fluids and ion transport, and inhibiting the metabolic processes [34].

Table 1: Antibacterial activity of TiO_2 NPs prepared without and with external magnetic field in deionized water by laser ablation at 60 mJ 1000 pulse.

Pathogens	Zone of inhibition (mm) TiO_2 NPs				
	Control	Without magnetic field		With magnetic field	
		A1	A2	B1	B2
Escherichia coli	0	26.1	32.3	34.2	33.1
Staphylococcus aureus	0	24.2	29.4	34.5	35.1

4. Conclusion

We have used magnetic field –assisted laser ablation in liquid (MFALAL) technique to prepared TiO_2 nanoparticles. The FE-SEM and TEM images confirmed that the prepared titanium oxide nanoparticles at B = 0 have spherical shape with average size of 25nm, while the TiO_2 nanoparticles prepared under effect of external magnetic field have mixed of platelets and nanowires morphology. XRD investigation revealed that the structure of TiO_2 nanoparticles prepared without magnetic field was anatase, while the XRD pattern of TiO_2synthesized with magnetic field was mixed of anatase and rutile as well as applying of the magnetic field improved the crystallinity of the nanoparticles. UV-Vis spectroscopy revealed that optical absorbance of the nanoparticles was found to be increased after applying the magnetic field and the energy gap of TiO_2 nanoparticles decreased from 4.6 to 3.4 eV when an external magnetic field applying during the preparation of the nanoparticles. Raman results show the presence of six vibration modes namely, E_g , B_{1g}, E_g, B_{1g} , A_{1g}, and B_{2g} and the intensity of the Raman peaks was increased after applying an external magnetic field during the ablation of TiO_2 nanoparticles. Antibacterial effect of TiO_2 nanoparticles prepared under effect of external magnetic field have toxic effect is greater than that of the particles produced without the influence of the magnetic field for the both types of bacteria (*E. coli* and *S. aureus*).

Declarations

Conflict of Interest

The authors have declared no conflict of interest

References

[1] Shi, X., Yang, X., Wang, S., Wang, S., Zhang, Q., Wang, Y.: Photocatalytic degradation of rhodamine B dye with MWCNT/TiO 2/C 60 composites by a hydrothermal method. J. Wuhan Uni. Technol. Mater. Sci. Ed. 26(1), 65-69. (2011).

[2] Barreca, F., Acacia, N., Barletta, E., Spadaro, D., Curro, G., Neri, F.: Titanium oxide nanoparticles prepared by laser ablation in water. Radiat. Eff. Def. Solids: Incorp. Plasma Sci. Plasma Technol., 165(6-10), 573-578 (2010).

[3] MalekshahiByranvand, M., NematiKharat, A., Fatholahi, L., MalekshahiBeiranvand, Z.: A review on synthesis of nano-TiO2 via different methods. J.nanostruct., 3(1), 1-9. (2013).

[4] Bahrami, A., Delshadi, R., Assadpour, E., Jafari, S. M., & Williams, L. (2020). Antimicrobial-loaded nanocarriers for food packaging applications. *Advances in Colloid and Interface Science*, 102140.

[5] Yousefi, M., Ehsani, A., & Jafari, S. M. (2019). Lipid-based nano delivery of antimicrobials to control food-borne bacteria. *Advances in colloid and interface science*, *270*, 263-277.

[6] Khashan, K. S., Sulaiman, G. M., Hussain, S. A., Marzoog, T. R., & Jabir, M. S. (2020). Synthesis, Characterization and Evaluation of Anti-bacterial, Anti-parasitic and Anti-cancer Activities of Aluminum-Doped Zinc Oxide Nanoparticles. *Journal of Inorganic and Organometallic Polymers and Materials*, 1-17.

[7] Khashan, K. S., Sulaiman, G. M., Abdul Ameer, F. A. K., & Napolitano, G. (2016). Synthesis, characterization and antibacterial activity of colloidal NiO nanoparticles. Pakistan journal of pharmaceutical sciences, 29(2).

[8] Sulaiman, G. M., Tawfeeq, A. T., & Jaaffer, M. D. (2018). Biogenic synthesis of copper oxide nanoparticles using olea europaea leaf extract and evaluation of their toxicity activities: An in vivo and in vitro study. Biotechnology progress, 34(1), 218-230.

[9] Khashan, K. S., Sulaiman, G. M., Hussain, S. A., Marzoog, T. R., & Jabir, M. S. (2020). Synthesis, Characterization and Evaluation of Anti-bacterial, Anti-parasitic and Anti-cancer Activities of Aluminum-Doped Zinc Oxide Nanoparticles. *Journal of Inorganic and Organometallic Polymers and Materials*, 1-17.

[10] Ismail, R. A., Sulaiman, G. M., Abdulrahman, S. A., & Marzoog, T. R. (2015). Antibacterial activity of magnetic iron oxide nanoparticles synthesized by laser ablation in liquid. Materials Science and Engineering: C, 53, 286-297.

[11] Russo, P., Liang, R., He, R. X., Zhou, Y. N.: Phase transformation of TiO_2 nanoparticles by femtosecond laser ablation in aqueous solutions and deposition on conductive substrates. Nanoscale, 9(18), 6167-6177. (2017)

[12] Song, Y., Yang, Y., Medforth, C.J., Pereira, E., Singh, A.K., Xu, H., Jiang, Y., Brinker, C.J., van Swol, F. Shelnutt, J.A.: Controlled synthesis of 2-D and 3-D dendritic platinum nanostructures. J. American Chem. Soc., 126(2), 635-645. (2004)

[13] Singh, A., Vihinen, J., Frankberg, E., Hyvarinen, L., Honkanen, M., Levanen, E.: Pulsed laser ablation-induced green synthesis of TiO_2 nanoparticles and application of novel small angle X-ray scattering technique for nanoparticle size and size distribution analysis. Nanoscale Res. Lett., 11(1), 1-9. (2016)

[14] Colon, G., Hidalgo, M. C., Navio, J. A.: A novel preparation of high surface area TiO_2 nanoparticles from alkoxide precursor and using active carbon as additive. Catalysis today, 76(2-4), 91-101. (2002)

[15] Shakhatov, V. A., Gordeev, O. A.: Thin film deposition by means of laser ablation of titanium oxide targets in oxygen radiofrequency electrode plasma. High Energy Chem., 42(2), 141-144. (2008)

[16] Solati, E., Aghazadeh, Z., Dorranian, D.: Effects of liquid ablation environment on the characteristics of TiO_2 Nanoparticles. J ClustSci , 31(5), 961-969 (202

[17] Nath, A., Laha, S. S., Khare, A.: Synthesis of TiO_2 nanoparticles via laser ablation at titanium-water interface. Integ. Ferro., 121(1), 58-64. (2010)

[18] Attan, N., Nur, H., Efendi, J., Lintang, H. O., Lee, S. L., Sumpono, I.: Well-aligned titanium dioxide with very high length-to-diameter ratio synthesized under magnetic field. Chem. Lett., 41(11), 1468-1470. (2012)

[19] Raid A.Ismail ,Ghassan M.Sulaiman, Safa A.Abdulrahman .: Antibacterial activity of magnetic iron oxide nanoparticles synthesized by laser ablation in liquid., 53, 286-297. (2015)

[20] Kareem H. Jawad, Buthenia A. Hasoon, Nehia N. Hussein., Biological application of titanium dioxide nanoparticles prepared through laser ablation in liquid., Drug Invention Today , 12, 10 . (2019)

[21] Giorgetti, E., Miranda, M. M., Caporali, S., Canton, P., Marsili, P., Vergari, C., Giammanco, F.: TiO_2 nanoparticles obtained by laser ablation in water: influence of pulse energy and duration on the crystalline phase. J. Alloy. Compd., 643, S75-S79. (2015).

[20] Meagher E P, Lager G A.:Polyhedral thermal expansion in the TiO_2 polymorphs: refinement of the crystal structures of rutile and brookite at high temperature, The Canadian Mineralogist, 17, 77-85. (1979)

[21] H. Seki, N. Ishizawa, N. Mizutani and M. Kato: High temperature structures of the rutile-type oxides, TiO_2 and SnO_2. Yogyo Kyokai Shi. *J. Ceramic Assoc. of Japan* 92, 219 (1984).

[22] Ma, C., Tschauner, O., Beckett, J. R., Rossman, G. R., Liu, W.: Panguite $(Ti^{4+}, Sc, Al, Mg, Zr, Ca)_{1.8}\ O_3$, a new ultra-refractory titania mineral from the Allende meteorite: Synchrotron micro-diffraction and EBSD. American Mineralogist, 97(7), 1219-1225. (2012)

[23] Fusi, M., Russo, V., Casari, C. S., Bassi, A. L., Bottani, C. E.: Titanium oxide nanostructured films by reactive pulsed laser deposition. Appl. Surf. Sci., 255(10), 5334-5337. (2009).

[24] Ismail, R. A., Mousa, A. M., Khashan, K. S., Mohsin, M. H., & Hamid, M. K. Synthesis of PbI_2 nanoparticles by laser ablation in methanol. Journal of Materials Science: Materials in Electronics, 27(10), 10696-10700. (2016).

[25] Zhang, J., Zhou, P., Liu,P., Yu,J.: New understanding of the difference of photocatalytic activity among anatase, rutile and brookite TiO_2 *Phys. Chem. Chem. Phys.*, 16, 20382-20386 (2014)

[26] Ismail, R. A., Abdulrazaq, O. A., Yahya, K. Z. Preparation and characterization of In_2O_3 thin films for optoelectronic applications. Surf. Rev. Lett., 12(04), 515-518. (2005).

[27] Ismail, R. A., Sulaiman, G. M., Abdulrahman, S. A. Preparation of iron oxide nanoparticles by laser ablation in DMF under effect of external magnetic field. Internat.J. of Modern Phys. B, 30(17), 1650094. (2016)

[28] Ismail, R. A., Almashhadani, N. J., Sadik, R. H.: Preparation and properties of polystyrene incorporated with gold and silver nanoparticles for optoelectronic applications. Appl. Nanosci., 7(3-4), 109-116. (2017)

[29] E. Salim et al., Effect of light induced heat treatment on the structural and morphological properties of $LiNbO_3$ thin films, Superlattices and Microstructures 128, 67–75. (2019)

[30] Ismail, R. A., Khashan, K. S., Mahdi, R. O. Characterization of high photosensitivity nanostructured 4H-SiC/p-Si heterostructure prepared by laser ablation of silicon in ethanol. Mater. Sci. Semiconduct. Process., 68, 252-261. (2017)

[31] Wypych, A., Bobowska, I., Tracz, M., Opasinska, A., Kadlubowski, S., Krzywania-Kaliszewska, A., Grobelny, J. Wojciechowski, P., Dielectric properties and characterization of titanium dioxide obtained by different chemistry methods. J. Nanomater., 124814. (2014).

[32] Wang, L., Hu, C., & Shao, L.: The antimicrobial activity of nanoparticles: present situation and prospects for the future. *International journal of nanomedicine*, *12*, 1227–1249. (2017).

[33] Jiang, J., Pi, J., & Cai, J. ,:The advancing of zinc oxide nanoparticles for biomedical applications. Bioinorganic chemistry and applications,: national library of medicine. 1062562. (2018).

[34] Al Rugaie, O., Jabir, M., Kadhim, R., Karsh, E., Sulaiman, G. M., Mohammed, S. A., ... & Mohammed, H. A. ,:Gold Nanoparticles and Graphene Oxide Flakes Synergistic Partaking in Cytosolic Bactericidal Augmentation: Role of ROS and NOX_2 Activity. Microorganisms, 9(1), 101. (2021).

Figures

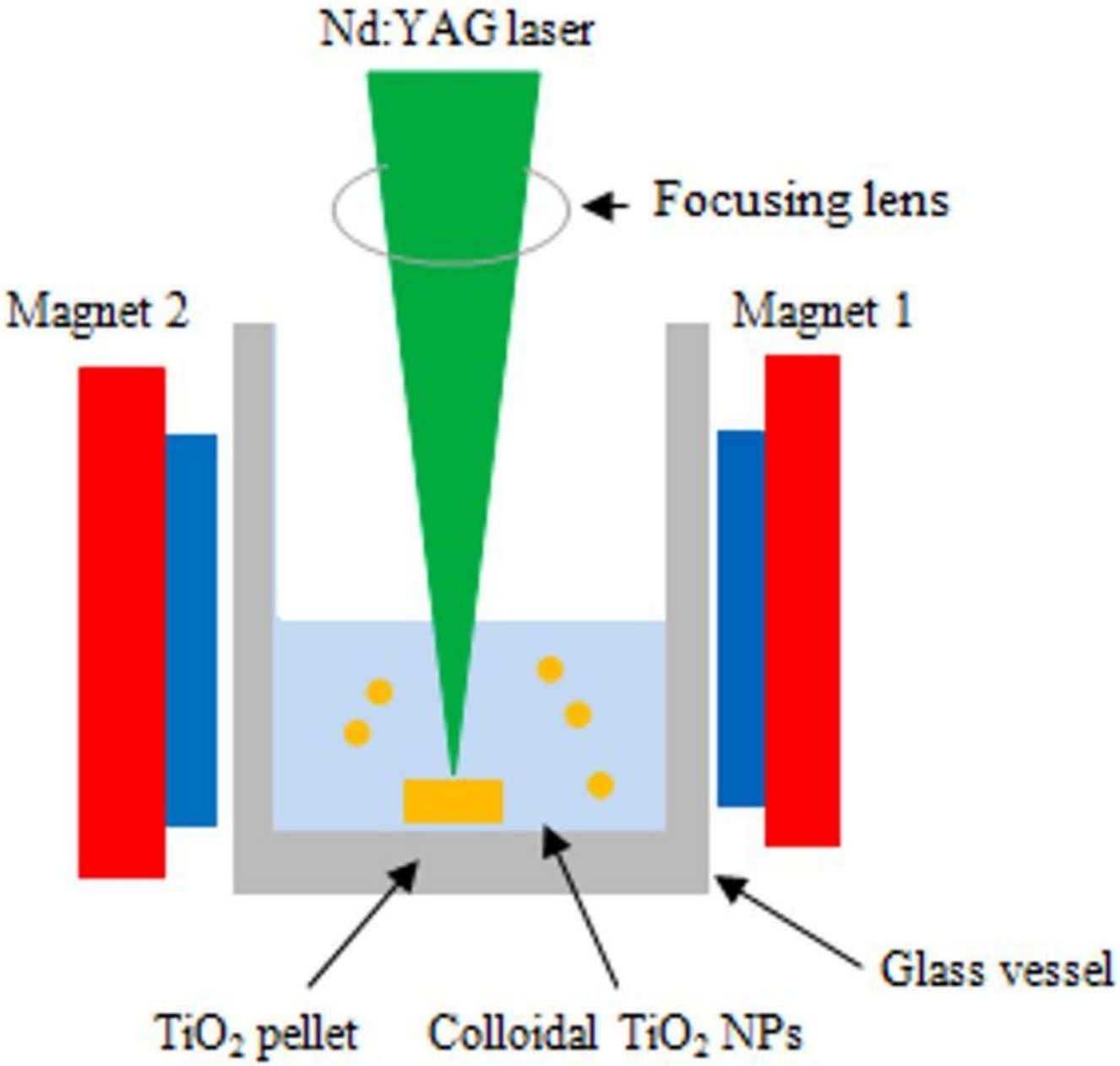

Figure 1

Schematic illustration of magnetic field- assisted laser ablation experimental setup

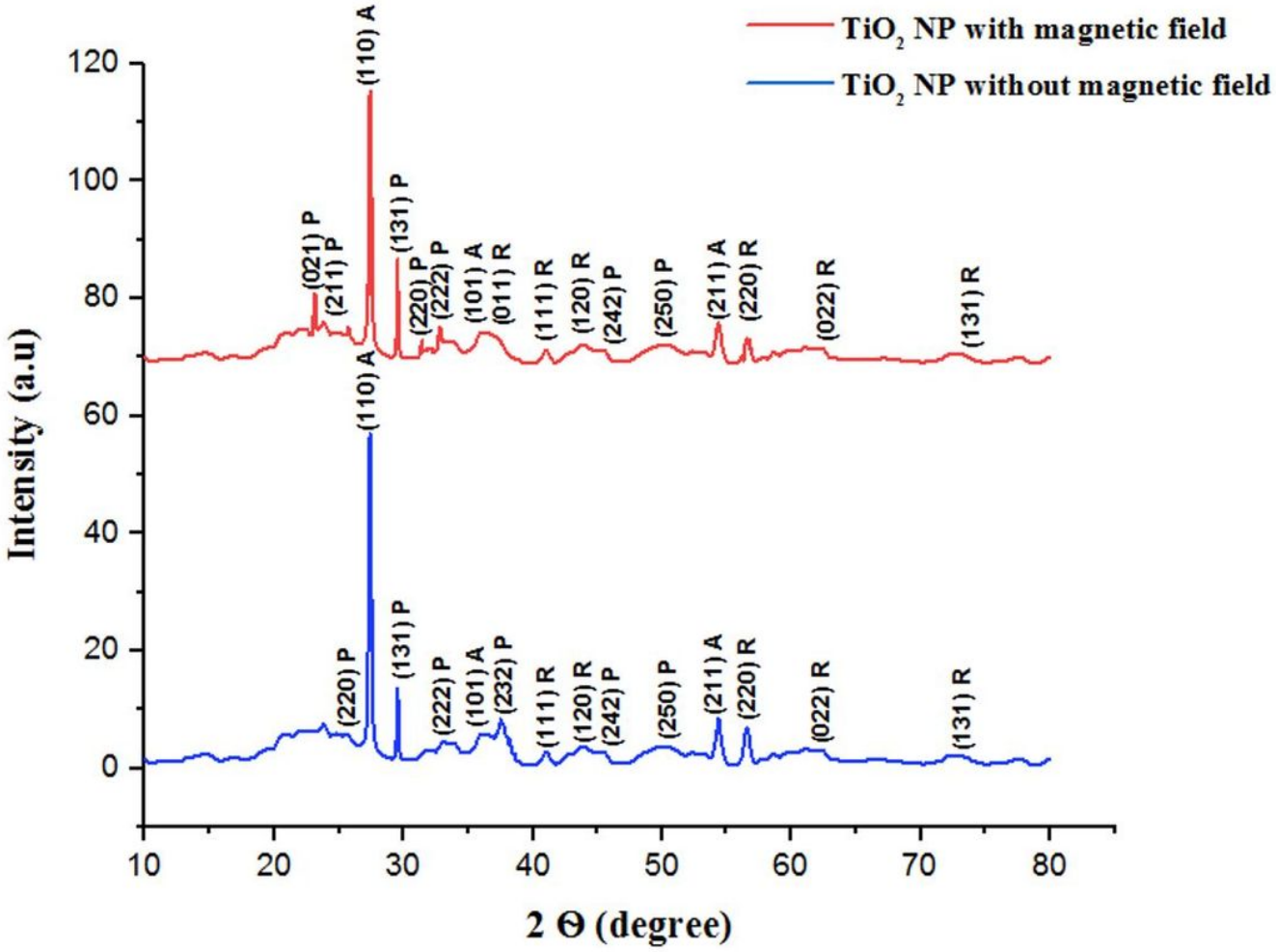

Figure 2

XRD patterns of TiO2 nanoparticles prepared without and with magnetic field

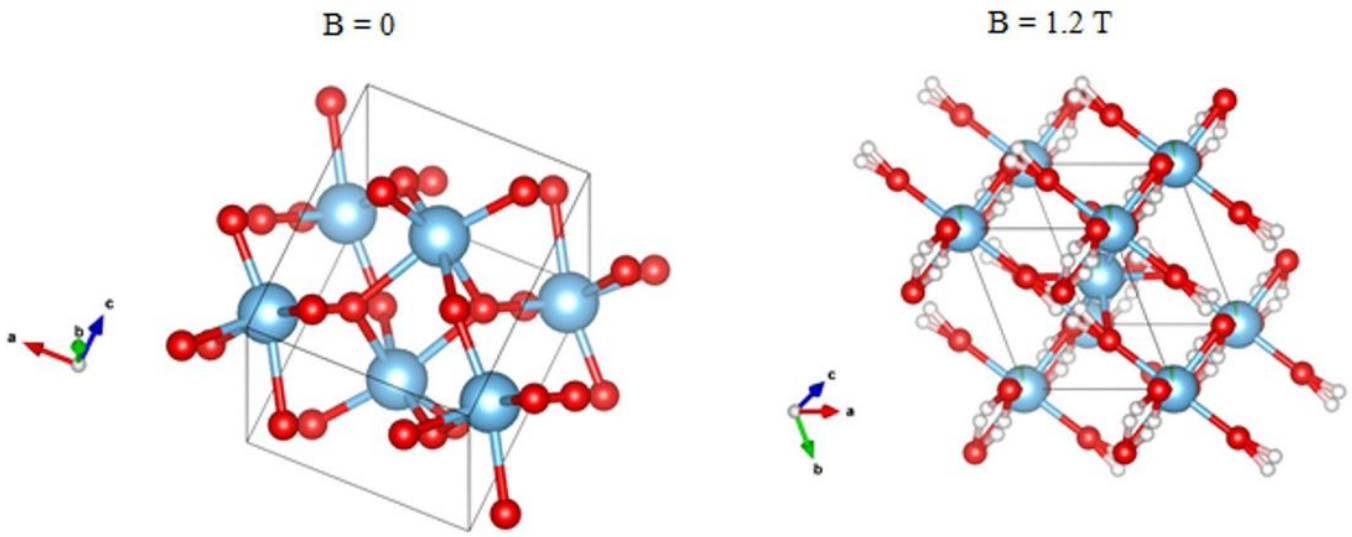

Figure 3

Crystal structure and crystal axis of TiO2 prepared at B=0 and B = 1.2T

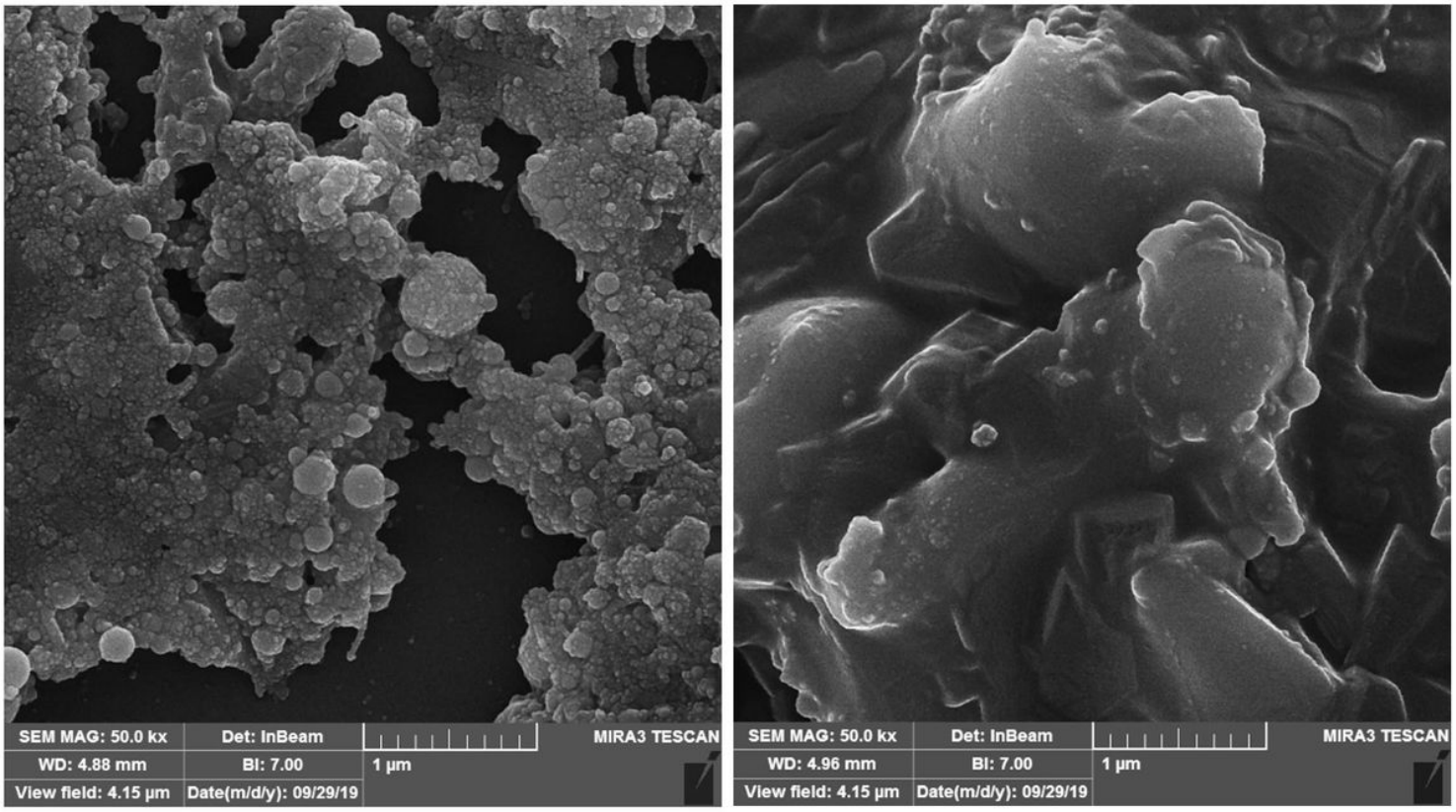

Figure 4

FESEM images of titanium oxide nanoparticles prepared (left) without applying magnetic field and (right) with magnetic field

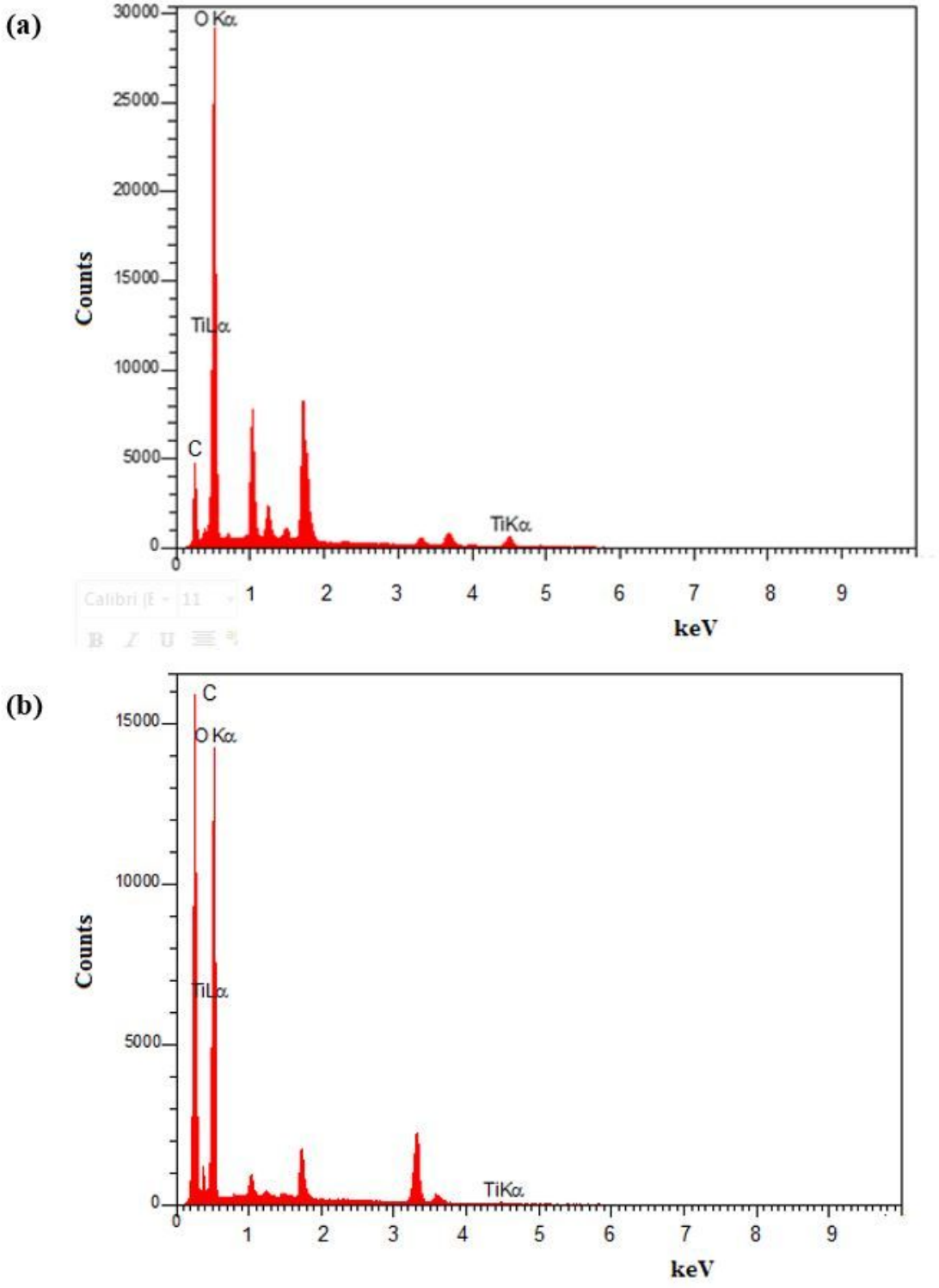

Figure 5

DEX spectrum of TiO2 prepared at (a) B = 0 (b) B = 1.2T

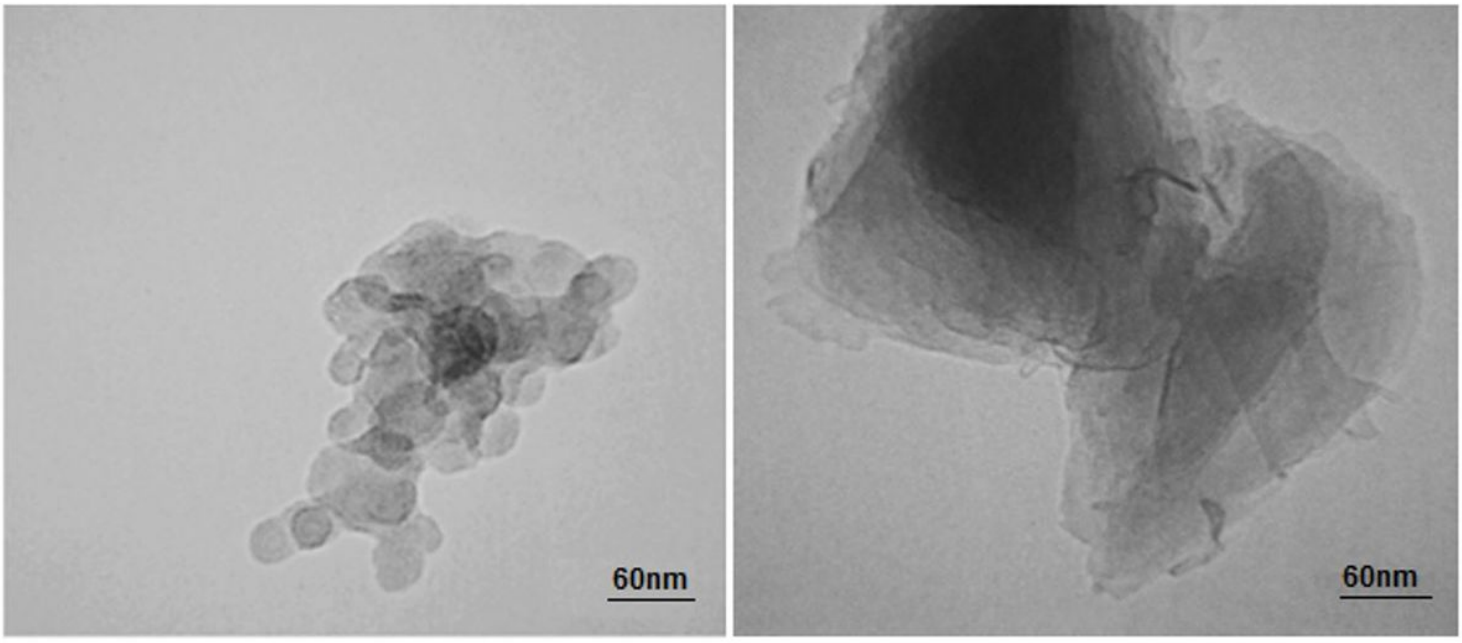

Figure 6

TEM images of titanium oxide nanoparticles prepared (left) without applying magnetic field and (right) with magnetic field

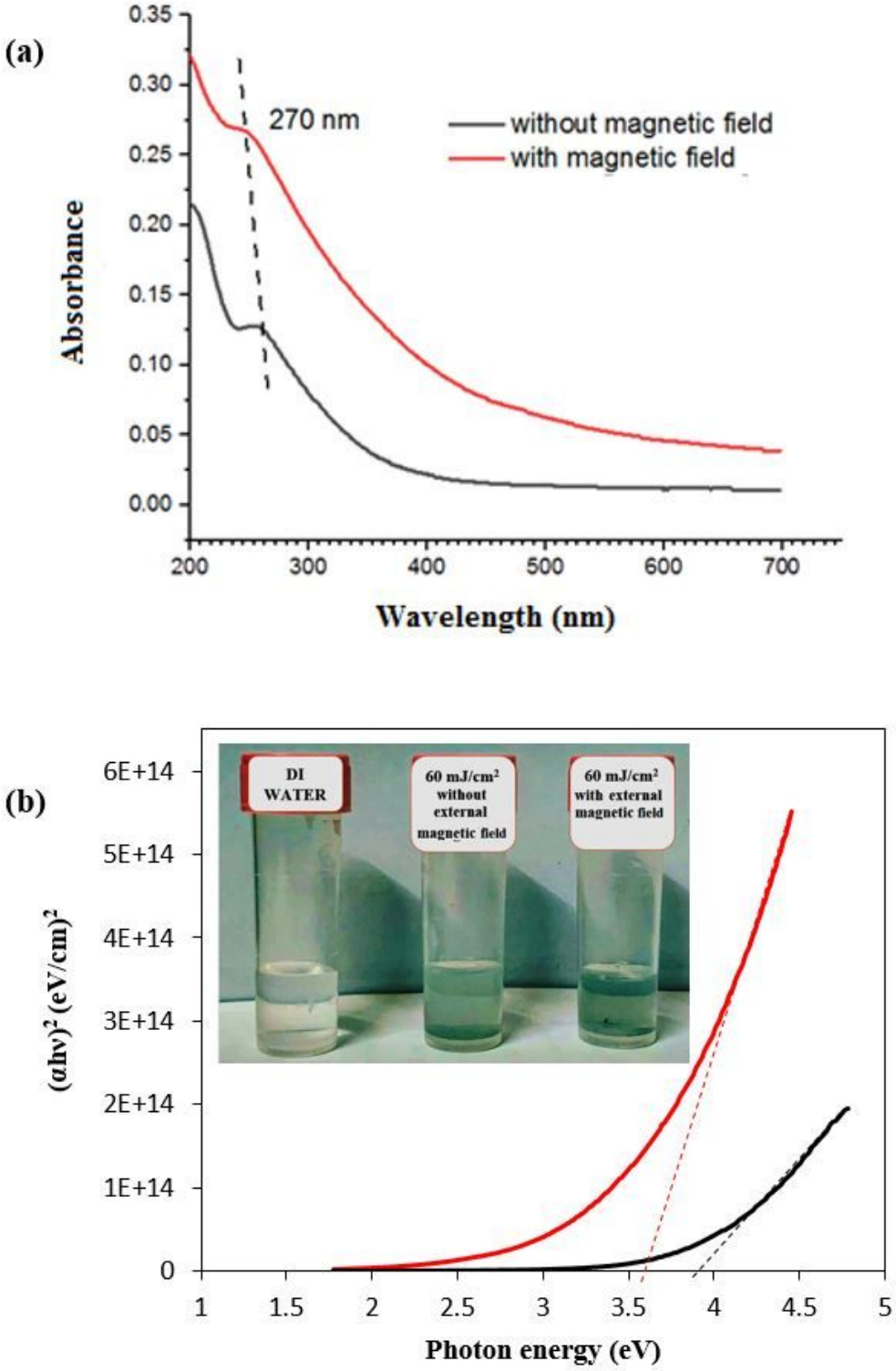

Figure 7

(a) Optical absorbance (a) (αhv)2 versus photon energy plot and (b) (αhv)0.5 versus photon energy of TiO2 nanoparticles prepared without and with magnetic field. Inset is the photographs of fresh prepared colloidal TiO2 nanoparticles with and without magnetic field

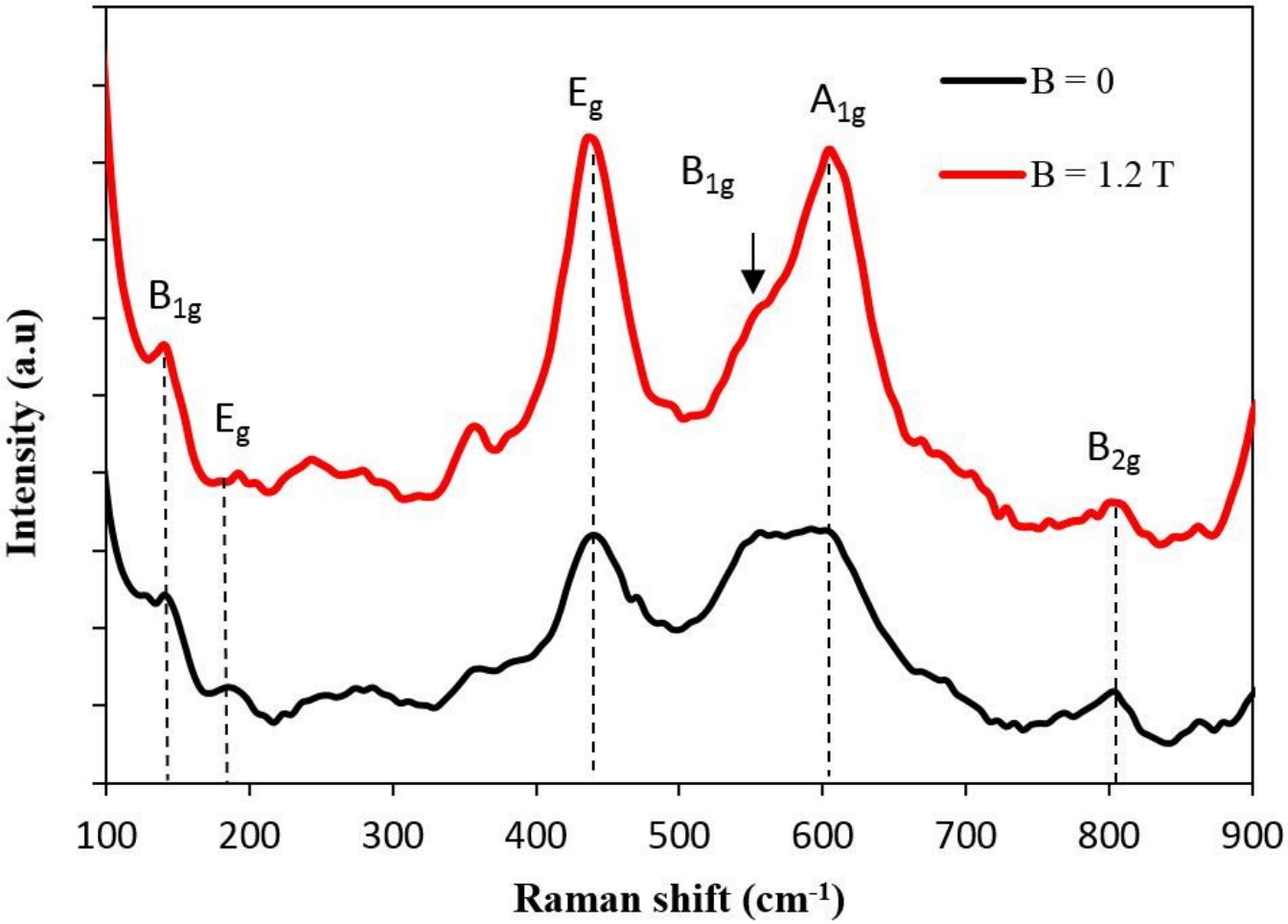

Figure 8

Raman spectra of TiO2 nanoparticles prepared with and without of magnetic field

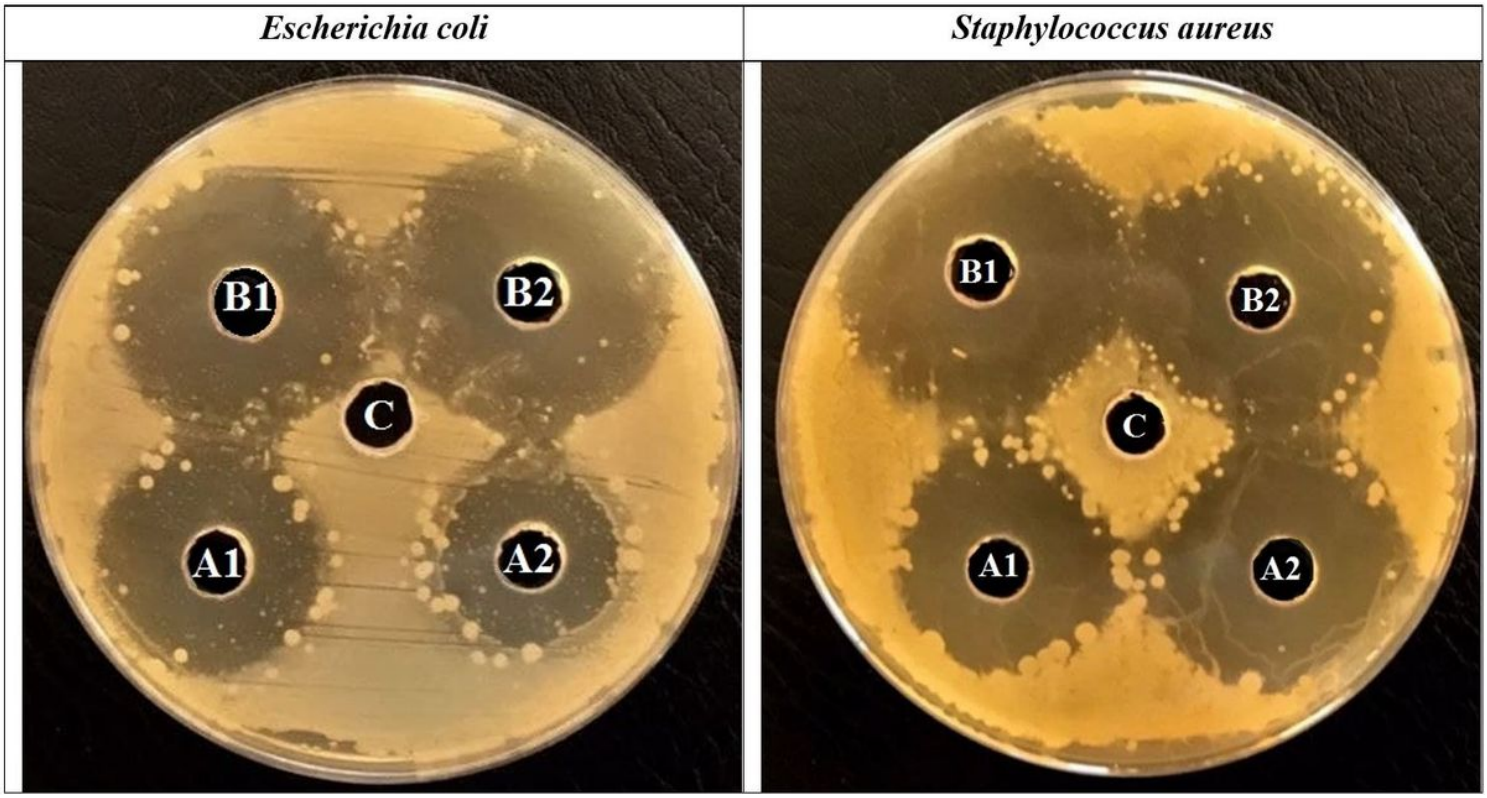

Figure 9

Antibacterial activity of titanium dioxide nanoparticles prepared in deionized water by laser ablation at 60 mJ and 1000 pulse (A: TiO2 NP prepared without the effect of external magnetic field. B: TiO2 NP prepared with effect of an external magnetic field).